

ANALYSIS OF A SOLAR SAIL MERCURY SAMPLE RETURN MISSION

Gareth W. Hughes^{*}, Malcolm Macdonald^{*}, Colin R. McInnes[†]

^{*}Research Assistant, Dept. of Aerospace Engineering, University of Glasgow, Glasgow, UK

[†]Professor, Department of Mechanical Engineering, University of Strathclyde, Glasgow, UK
ghughes@aero.gla.ac.uk, m.macdonald@aero.gla.ac.uk, colin.mcinnnes@strath.ac.uk

Alessandro Atzei, Peter Falkner

ESA/ESTEC, Science Payloads and Advanced Concepts Office, Noordwijk, The Netherlands
aatzei@rssd.esa.int, Peter.Falkner@esa.int

ABSTRACT

A conventional Mercury sample return mission requires significant launch mass, due to the large Δv required for the outbound and return trips, and the large mass of a planetary lander and ascent vehicle. Solar sailing can be used to reduce lander mass allocation by delivering the lander to a low, thermally safe orbit close to the terminator. In addition, the ascending node of the solar sail parking orbit plane can be artificially forced to avoid out-of-plane manoeuvres during ascent from the planetary surface. Propellant mass is not an issue for solar sails so a sample can be returned relatively easily, without resorting to lengthy, multiple gravity assists. A 275 m solar sail with an assembly loading of 5.9 g m^{-2} is used to deliver a lander, cruise stage and science payload to a forced Sun-synchronous orbit at Mercury in 2.85 years. The lander acquires samples, and conducts limited surface exploration. An ascent vehicle delivers a small cold gas rendezvous vehicle containing the samples for transfer to the solar sail. The solar sail then spirals back to Earth in 1 year. The total mission launch mass is 2353 kg, on an H2A202-4S class launch vehicle ($C_3=0$), with a ROM mission cost of 850 M€. Nominal launch is in April 2014 with sample return to Earth 4.4 years later. Solar sailing reduces launch mass by 60% and trip time by 40%, relative to conventional mission concepts.

INTRODUCTION

Mercury Science

Of the terrestrial planets, Mercury is the one of which we know the least, its location deep within the solar gravity well ensuring that spacecraft have been sent there infrequently. Mercury's unusual 3:2 spin-orbit resonance meant that the same side was imaged in each of the Mariner 10 flybys. Surface coverage is incomplete and the planet must be comprehensively mapped by an orbiter mission such as BepiColombo or Messenger, before a sample return mission can proceed and a landing site selected. There is no significant water or atmosphere, so that daytime temperatures can soar to 700 K, and plummet to 100 K at night, due to the slow spin period. The lack of CO_2 or H_2O in the atmosphere suggests that Mercury is either intrinsically volatile deficient, or is not out-gassing at a rate

comparable to that of the Earth, and so is less geologically active.¹ Aside from the Earth, Mercury is the only terrestrial planet which is known to have an intrinsic, weak, magnetic field. This is produced either by an Earth-like magnetohydrodynamic dynamo in the core, or a remnant magnetic field in the rock, which could be evident in any surface samples returned. The high average density of 5.43 g m^{-3} could be due to the presence of Iron within the interior, perhaps generated by this Earth-like magnetohydrodynamic dynamo, consistent with electrical currents flowing in a molten core. Tectonically, unique compressive thrust faults called lobate scarps occur on a global scale, implying global compressive stresses in Mercury's distant past. Large impact basins on Mercury can also contain volcanic deposits, which suggests that there has been volcanic activity after the impact. Little is known about the surface geology, composition, and chemistry, therefore sample

return would be of significant benefit. Radar reflection measurements appear to show volatile compounds, possibly water ice, at both poles, deep within the shadows of craters, but observations from Earth are difficult due to the proximity of Mercury to the Sun. The lack of any appreciable atmosphere means that very cold regions exist in polar craters, allowing radar-bright materials to remain.

Science Objectives

It is important to ascertain the surface age of Mercury to understand its geologic history. Accurate rock dating of Mercury surface samples is only possible on Earth. Due to the tenuous atmosphere, the entire descent must be via chemical propulsion. A high-latitude landing site is selected due to thermal constraints, and prior imaging of this site from the orbiter at a resolution of better than 1 metre per pixel is necessary. Even at high latitudes, landing in direct sunlight, or indeed in permanent shadow would be undesirable. A landing site within a suitable crater, in partial shade, but with some light reflected from the crater walls is preferable, with a sample drilled from a rock outcrop within the crater.² However, recent craters may be contaminated with material from their impactor, and should be avoided. Guided descent is employed for all but the last few metres of the descent, since the thruster plume would scorch the landing site, contaminating the surface regolith to be sampled. The stroke of the landing legs is used to absorb the remaining kinetic energy of surface impact.

Baseline science objectives for a Mercury sample return mission are therefore, to acquire a surface sample through a precision landing at a carefully selected high latitude landing site in partial shadow, within a suitably aged crater, with high resolution imaging for documentation during terminal descent. Sample pre-selection and pre-analysis will be conducted in-situ during landing site characterisation using a robotic arm and small mobility device (20 m range).¹ The primary science goal is to acquire 350 g of surface regolith. Mercury is not thought to be of direct interest to exobiology in the solar system, so planetary protection measures will be simpler than for Mars missions, more similar to lunar missions.

Solar Sailing

The extremely high Δv required for Mercury sample return can be met relatively easily by solar sails, since propellant mass is not an issue, significantly reducing launch mass. Lengthy multiple gravity assists are not required, and the launch window is always open in principle. Thermally-safe orbit precession at Mercury is possible using the continuous thrust. Solar sail performance is defined by the Characteristic Acceleration, the solar radiation pressure induced acceleration at 1 AU with the sail normal oriented along the Sun-line.³

PAYLOAD MODEL

A full and detailed solar sail payload has been defined and customised,⁴ based loosely on an internal ESA Assessment Study,¹ with some aspects drawn from a NASA/JPL Team X report.² A trade-off of the optimum solar sail parking orbit at Mercury was conducted so as to minimise the Mercury Ascent Vehicle (MAV) Δv requirements. The use of an artificial Sun-Synchronous polar orbit at Mercury close to the planetary terminator,⁵ can be effected to reduce the thermal loads on the orbiter through a constant precession of the line of nodes, enabling a longer orbiter stay time and much lower parking orbit. The characteristic acceleration of the sail in the parking orbit is defined by the parameters of the Sun-Synchronous orbit, and so as the acceleration is increased the Sun-Synchronous orbit can be increasingly circularised. Fig. 1 shows the effect of rendezvous orbit altitude on MAV launch mass. It is seen that ascent direct to the Sun-Synchronous orbit requires much more Δv than ascent to a circular orbit. A circular 100 km orbit was selected to minimise MAV Δv requirements, with the sail used to deliver the lander onto the 100 km orbit, after an initial 44 day science and landing site selection phase on a 100 x 7500 km forced Sun-Synchronous orbit, 10° ahead of the solar terminator. During sample acquisition, until after coplanar MAV launch, the sail rotates the circular 100 km orbit plane to rendezvous with the MAV orbit, before spiralling to escape.

The solar sail payload stack comprises a small cold-gas Sail Rendezvous Vehicle

(SRV), to conduct proximity manoeuvres when transferring the sample from the MAV to the ballistic Earth Return Vehicle (ERV) attached to the Sail Cruise Stage (SCS). The bi-propellant MAV and cold-gas SRV is mounted on the bi-propellant Mercury Descent Vehicle (MDV). The MDV has a large science platform and 0.4 m^2 Gallium Arsenide solar arrays. Fig. 2 shows the lander deployed with its landing legs extended. Tables 1-4 show the mass breakdown of the SRV, MAV, MDV, and SCS, respectively. An analysis of the spacecraft subsystems, shows a total spacecraft mass of 1905 kg, to support acquisition of 350 g of surface samples.

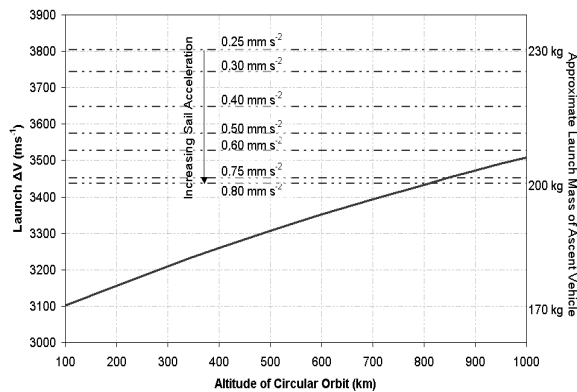


Figure 1: Mercury Ascent Vehicle rendezvous orbit trade-off (solid line: ascent to circular orbit, dashed lines: ascent to elliptical Sun-Synchronous orbit)

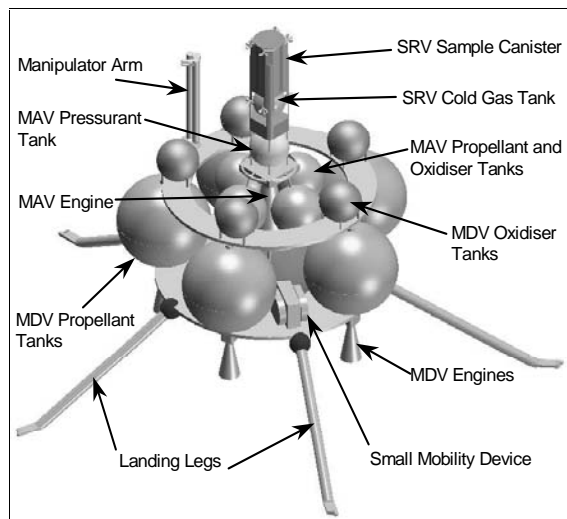


Figure 2: Mercury Sample Return lander

The SRV has a 2 kg sample container which holds the surface samples, with 50 m s^{-1} of propellant allocated for the rendezvous manoeuvre. The MAV uses a single stage DASA S3K class bi-propellant MMH/MON-3 engine, with a specific impulse of 352 s. However, volume reductions and an increase in thrust to 4 kN would be necessary. The MDV uses 5 bi-propellant MMH/MON-3 engines, delivering 6 kN each with a specific impulse of 320 s. The SCS allows for on-orbit power generation via 6.25 m^2 Gallium Arsenide solar arrays. The SCS telecommunications system comprises low and medium-gain X-band systems, a high-gain X/Ka band system, and a UHF link with the lander. The telecommunications systems have been sized to ensure adequate data return for the mission. A 28 volt, three domain, regulated power system is used. The SCS requires 332 W in Sunlight and 310 W during eclipse, met by $365 \text{ W } 6.25 \text{ m}^2$ GaAs solar arrays, and 349 Wh Lithium-Ion batteries. The MDV requires 71 W, met through a 78 W 0.4 m^2 GaAs solar array. The 56 W MAV power requirement is attained through 53 Wh Li-Ion batteries. The SRV requires 24 W, provided by a 221 Wh Li-Ion battery over the SRV operational lifetime. The ballistic Earth Return Vehicle (ERV) uses a 41 Wh Primary Lithium battery to provide 1.7 W of power.

Science Instruments

The on-orbit SCS science payload includes a High Resolution Stereo Camera (10 W, 10-100 bps), Laser Altimeter (10 W, <1 bps), Infra-Red Radiometer (5 W, 100-5000 bps), X-ray Fluorescence Spectrometer (10 W, 100-2000 bps), Radio Science Instruments (5 W, 10-100 bps), and associated high-capacity memory (5 W, 2-5 Gbytes). There is also an 8 kg allocation for a payload of opportunity (10 W, 5 kbps).

The lander has science instruments and manipulator hardware mounted on the MDV, which include a Sampling Device, Robotic Arm, and a small Rover vehicle. The total data rate of these instruments corresponds to 92 Mbit every 10 hours, with a total power consumption of 11.8 W.

SRV Component	Mass (kg)	Contingency (%)	Total mass (kg)
Sample container	2.0	-	2.0
SRV Payload Mass	2.0	-	2.0
Attitude control	3.1	10	3.4
Command & data	0.5	10	0.6
Power	2.0	10	2.2
Mechanisms	0.1	10	0.1
Telecomms	1.1	10	1.2
Thermal	1.0	10	1.1
Structure	2.0	10	2.2
SRV Bus Mass	9.8	10	10.9
Thrusters	0.2	15	0.23
Valves, pipes	0.1	15	0.1
Propellant tank	0.1	15	0.1
Propulsion Mass (Dry)	0.4	15	0.43
SRV Dry Mass	12.2		13.3
System contingency	-	1	0.1
Total SRV Dry Mass			13.4
Propellant for rendezvous	1.0	15	1.1
Total SRV Mass (Wet)			14.5

Table 1: Sail Rendezvous Vehicle (SRV) system sheet mass breakdown

MAV Component	Mass (kg)	Contingency (%)	Total mass (kg)
SRV	14.5	-	14.5
MAV Payload Mass	14.5	-	14.5
Attitude control	4.5	10	4.9
Command & data	2.5	10	2.7
Power	2.3	10	2.5
Mechanisms	0.5	10	0.6
Telecomms	0.0	10	0.0
Thermal	2.0	10	2.2
Structure	5.2	10	5.7
MAV Bus Mass	17.0	10	18.6
Thruster	15.0	15	17.3
Valves, pipes	2.9	15	3.3
Propellant tank	9.5	15	10.9
Propulsion Mass (Dry)	27.4		31.5
MAV Dry Mass	58.9		64.6
System contingency	-	1	0.65
Total MAV Dry mass			65.3
Propellant for ΔV_1	0.5	15	0.6
Propellant for ΔV_2	94.8	15	109.0
Total Propellant Mass	95.29	15	109.6
Total MAV Mass (Wet)			174.9

Table 2: Mercury Ascent Vehicle (MAV) system sheet mass breakdown

MDV Component	Mass (kg)	Contingency (%)	Total mass (kg)
MAV	174.9	-	174.9
Surface instruments	2.9	-	2.9
MDV Payload Mass	177.8		177.8
Attitude control	15.0	10	16.5
Command & data	4.0	10	4.4
Power	8.8	10	9.7
Mechanisms	22.0	10	24.2
Telecomms	0.0	10	0.0
Thermal	3.0	10	3.3
Structure	83.0	10	91.3
MDV Bus Mass	135.8	10	149.4
Thrusters (5 of 6kN)	50.0	15	57.5
Valves, pipes	8.3	15	9.5
Propellant Tanks	83.0	15	95.5
Propulsion Mass (Dry)	141.3	15	162.5
MDV Dry Mass	454.9		489.7
System contingency	-	1	4.9
Total MDV Dry Mass			494.6
Propellant for ΔV_1	4.0	15	4.6
Propellant for ΔV_2	830.8	15	955.4
Total Propellant Mass	834.8	15	960.0
Total MDV Mass (Wet)			1454.6

Table 3: Mercury Descent Vehicle (MDV) system sheet mass breakdown

SCS Component	Mass (kg)	Contingency (%)	Total mass (kg)
Lander (SRV/MAV/MDV)	1454.6	-	1454.6
Science payload	31.6	-	31.6
ERV	16.5	5	17.3
SCS Payload Mass	1502.7		1503.5
Attitude control	14.1	10	15.5
Command & data	10.0	10	11.0
Power	40.2	10	44.2
Mechanisms	161.0	10	177.1
Telecomms	24.6	10	27.1
Thermal	50.0	10	55.0
Structure	65.4	10	71.9
SCS Bus Mass	365.3	10	401.8
Total Sail Payload Mass			1905.3

Table 4: Sail Cruise Stage (SCS) system sheet mass breakdown

SOLAR SAIL SIZING

A square solar sail is envisaged, using tip-vanes for attitude control, sized to provide adequate slew rates for the planet-centred mission phases. The spacecraft (sail payload) is mounted centrally, within the plane of the solar sail, so that both faces of the core structure are free to be used as attachment points for the lander, and Earth return capsule. Fig. 3 shows approximate trip times from Earth to Mercury, generated using methods described in the Trajectory Analysis section. An outbound trip time of 2-3 years is desirable to be competitive with SEP and Chemical Mercury trip times. This is enabled by a characteristic acceleration of 0.25 mm s^{-2} . The chosen sail conceptual design used in this paper is based on the AEC-ABLE Scaleable Solar Sail Subsystem (S^4), since it can be extrapolated to large sail dimensions.⁶ This design is based on Coilable booms, and the boom linear density as a function of length can be combined with NASA/LaRC/SRS $2 \mu\text{m}$ or $5 \mu\text{m}$ CP1 film to obtain the sail assembly loading as a function of sail side length, shown in Fig. 4. It is assumed that conventional coatings are used, with Aluminium (85% reflectivity) on the frontside and Chromium (64% emissivity) on the backside. Fig. 4 also shows the necessary sail assembly loading as a function of sail side length, for delivery of a 1905 kg spacecraft to Mercury with a characteristic acceleration of 0.25 mm s^{-2} .

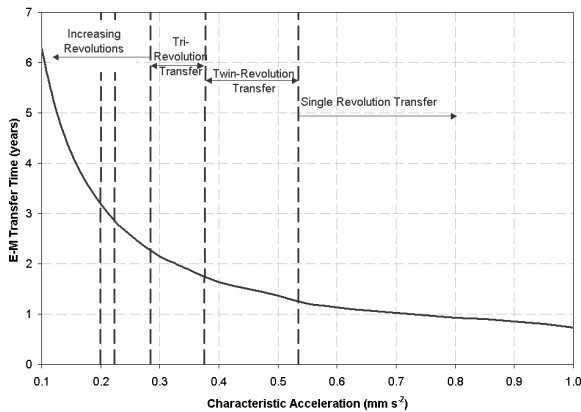


Figure 3: Approximate Earth-Mercury transfer time

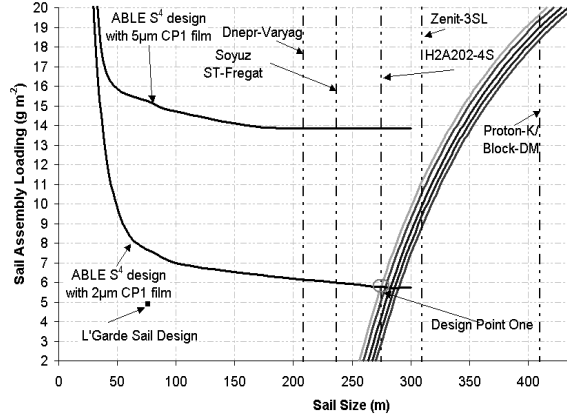


Figure 4: 0.25 mm s^{-2} solar sail design space (sail payload contours represent increasing parking orbit radius, with baseline 100 km orbit leftmost)

It can be seen that the intersection of the $2 \mu\text{m}$ CP1 ABL S^4 sail design curve with the 0.25 mm s^{-2} , 100 km orbit payload curve yields the sail design point, with an assembly loading of 5.9 g m^{-2} and sail dimensions of $275 \times 275 \text{ m}$. The design point and resultant characteristic accelerations during different points in the mission, as the lander is deployed and sample is returned, are shown in Table 5. It is important to stress that for a specific solar sail, the acceleration will increase as the solar sail payload mass is reduced, through the jettison of used modules.

Parameter	Value
Sail Assembly loading (@ 40% contingency)	5.9 g m^{-2}
Sail side length	275 m
Sail area (@ $2 \mu\text{m}$ thickness)	75625 m^2
Boom length	194 m
Sail reflective efficiency	0.85
Characteristic Acceleration (Earth departure)	0.25 mm s^{-2}
Characteristic Acceleration (Sample acquisition)	0.7367 mm s^{-2}
Characteristic Acceleration (Mercury departure)	0.7839 mm s^{-2}

Table 5: Solar sail specifications and resultant characteristic acceleration during each phase

A 275 m sail with an assembly loading of 5.9 g m⁻² has a mass of 448 kg, with a mass budget as shown in Table 6. A linear boom density of 70 g m⁻¹ is required with 0.94 m diameter to maintain a factor of safety against buckling. The total launch mass is therefore 2353 kg, which enables the use of an H2A202-4S class launch vehicle to escape velocity. The spacecraft stack with stowed sail is depicted within the H2A fairing in Fig. 5.

Component	Mass (kg)
Total payload mass	1905
2µm CP1 film (@ 2.86 g m ⁻²)	216
0.1µm Al coating (@ 0.54 g m ⁻²)	41
Bonding (@ 10% coated mass)	26
Sail booms	54
(ABLE 0.94m booms @ 70 g m ⁻¹)	
Mechanical systems (@ 40% contingency)	111
Total sail assembly mass	448
Total mission launch mass	2353
H2A202-4S capacity to C₃ = 0	2600
Launch mass margin	247 kg (9.5 %)

Table 6: Solar sail design point data set

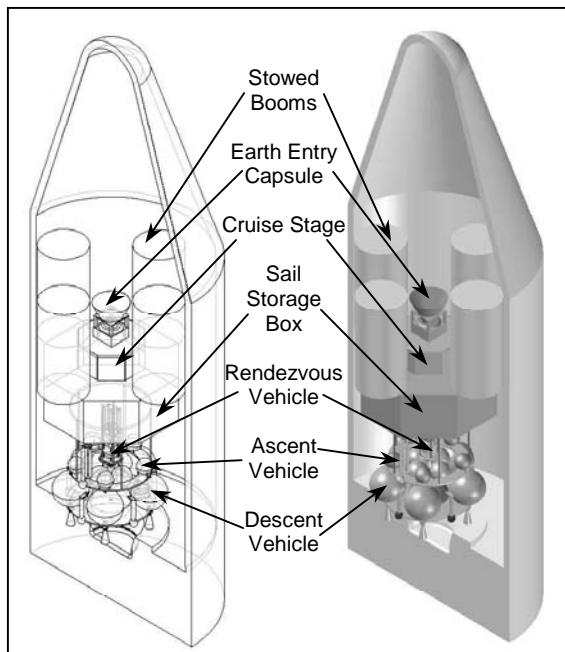


Figure 5: Payload stack in H2A 202-4S fairing

COST ANALYSIS

The spacecraft has been costed using parametric Cost Estimating Relationships (CERs).⁷ Conservative margins have been added, and the cost of specialist components, such as bi-propellant engines, have been taken from NASA/JPL Team X estimates.² Project management and integration and support costs are also estimated using Ref. 7. The most difficult system to cost is that of the solar sail, since a sail is yet to fly, let alone one of 275 m dimension. A crude estimate leads to a ROM cost of 28.4 M€, but it should be noted the cost of the sail is small in comparison with the spacecraft itself. In addition, the reduction in launch cost compared with conventional concepts more than makes up for sail cost.

Conservative cost margins of 30% have been added to give the mission cost breakdown shown in Table 7. The total solar sail Mercury sample return mission ROM cost is therefore of order 850 M€. We note that, although the launch cost is fairly low, the predominant cost component is the spacecraft itself, which is mostly independent of the primary propulsion method used. Traditionally, solar sailing is seen to be superior to chemical propulsion or SEP, if it can reduce launch mass and cost, but for a sample return mission, the sail must *significantly* reduce launch mass, for there to be any appreciable reduction in overall mission cost.

Component	Cost (FY03M€)	Margin (%)	Total Cost (FY03M€)
SRV	27.8	30	36.1
MAV	58.8	30	76.4
MDV	88.3	30	114.8
SCS	89.1	30	115.8
SOLAR SAIL	28.4	30	36.9
EEV	4.2	30	5.5
Spacecraft Cost	296.6	-	385.5
IA&T	94.9	30	123.4
Program Level	156.3	30	203.2
GSE	19.6	30	25.5
LOOS	18.1	30	23.5
Launch Cost (H2A)	83.9	10	92.3
Associated Costs	372.8	-	467.9
Total Mission Costs	669.4	-	853.4

Table 7: Cost breakdown

TRAJECTORY ANALYSIS

The required Δv for direct ballistic transfer to a low Mercury parking orbit is of order 13 km s^{-1} . Chemical propulsion and Solar Electric Propulsion (SEP) both require a prolonged sequence of gravity assists to reduce launch mass. Mercury sample return from deep within the solar gravity well is one of the most energetically demanding mission concepts imaginable. However, propellant mass is not an issue here and the sail can spiral directly to the planet, making best use of the inverse square increase in Solar Radiation Pressure (SRP) at lower heliocentric radii. Many authors have recognised the benefit of solar sailing to reach Mercury, but this paper provides new data sets by considering both launch windows, and return trajectories.

Heliocentric trajectories have been optimised using the constrained parameter optimisation algorithm, NPSOL, based on Sequential Quadratic Programming (SQP).^{8,9} Engineering insight coupled with 'incremental feedback' methods were used to obtain initial guesses for optimisation. Planet centred manoeuvres are modelled using a set of blended analytical control laws.¹⁰ Mercury capture and escape trajectories have been generated mainly using a control law which maximises the rate of change of orbit energy. Many control laws are blended for Mercury-centred transfer manoeuvres.

Launch windows

Fig. 6 shows the Earth departure date scan for the selected characteristic acceleration of 0.25 mm s^{-2} , over a 3 year period. Each point on the curve represents an optimisation at that launch date. It is seen that the minimum time launch opportunities occur once every year. Solar sailing is not restricted to launch windows, but it is clear that a saving of 300 days can be achieved depending on launch date. The discontinuities posed problems when incrementing the launch date to find initial guesses for other launch dates. These discontinuities are due to the spacecraft 'just missing' the target and having to execute another revolution of the Sun to reach Mercury. To determine the optimal launch date, consideration must also be given to the

variation of the capture and escape times along Mercury's orbit, and the return Mercury-Earth phase. Since Mercury has an eccentricity of 0.2056, then the available SRP will vary over a Mercury year.¹¹ Approximate capture and escape times are shown in Fig. 7, for the accelerations specified in Table 5.

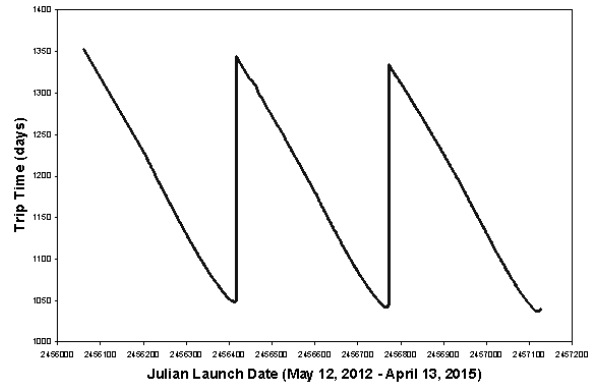


Figure 6: Earth-Mercury departure date scan

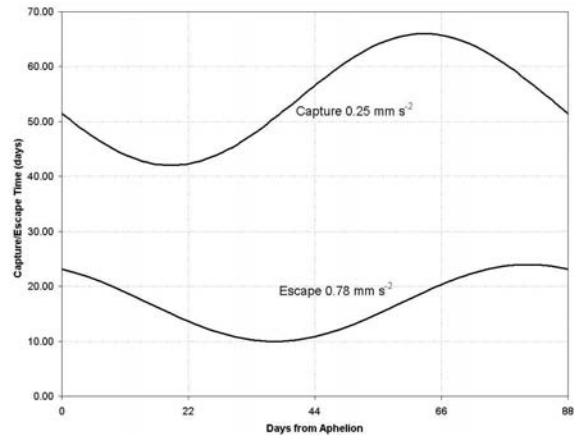


Figure 7: Mercury capture/escape time variation

With an orbiter stay time of order 40 days, Figs. 6 and 7 can be used to ascertain that the return scan was only required across a 2 year range (small variation). The 4 curves were then mapped together to determine the overall mission duration as a function of Earth departure date. This is shown in Fig. 8, where it is clear that the long duration outbound spiral dominates the total mission duration. The launch opportunity selected was that on April 19, 2014.

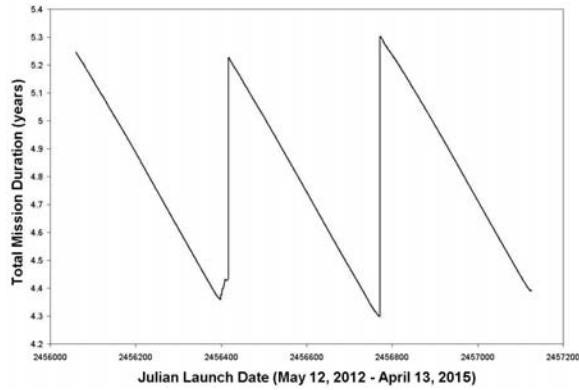


Figure 8: Total mission duration launch opportunities

Earth-Mercury Phase

The outbound trajectory is shown in Fig. 9, departing Earth with C_3 of zero on April 19, 2014. Mercury arrival is on February 24, 2017, 2.85 years later, after $5 \frac{1}{4}$ revolutions. The optimal cone and clock control angles are shown in Fig. 10. Even at a relatively coarse control resolution of 50 linear interpolation segments, the profiles are smooth and oscillatory.

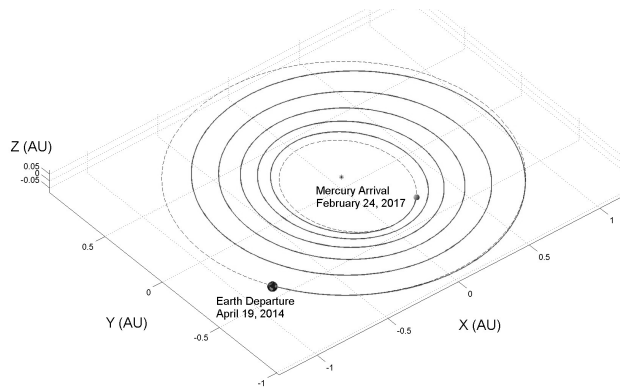


Figure 9: Earth-Mercury trajectory

The reduction in heliocentric radius and subsequent increase in sail film temperature is depicted in Fig. 11. Equilibrium sail film temperature is modelled using a black body approximation, assuming temperature changes take place instantaneously, since the micron-scale thickness of the film ensures that the thermal inertia is effectively zero. Aluminium/Chromium coatings are assumed

as was discussed previously. The temperature is a function of both the radius and the sail attitude, with a maximum value of 443.7 K. Even face on to the Sun at Mercury perihelion, the worst-case temperature would be 494.5 K, still less than the predicted 520 K upper limit of polyimide films.

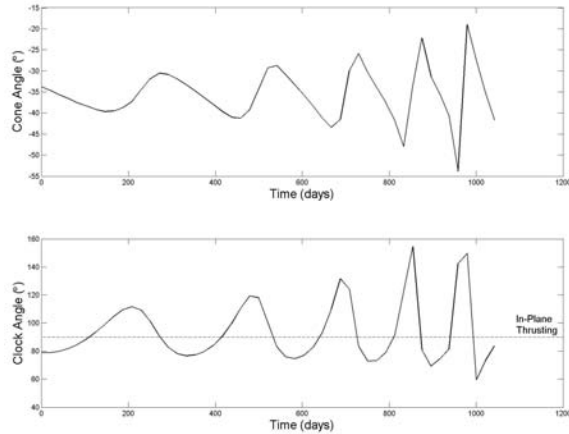


Figure 10: Earth-Mercury control angle profile

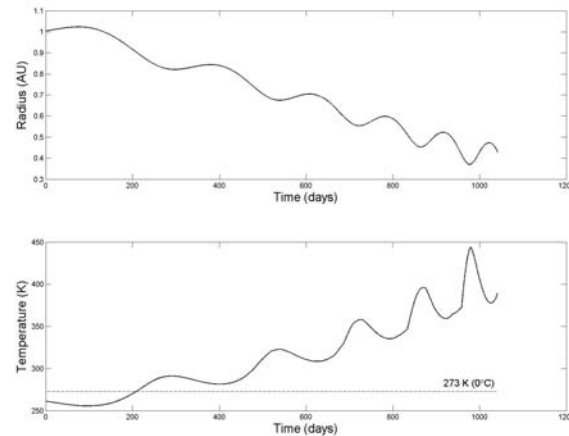


Figure 11: Earth-Mercury heliocentric radius and sail film temperature

Mercury Centred Manoeuvres

It has been assumed that the sail arrives at Mercury with zero hyperbolic excess velocity. The transition from heliocentric to planet-centred motion has not been patched. However, it is assumed that the sail can be used to correct for approach dispersion and can target the correct B-plane for capture. As

has been prescribed, capture is into a 100 km x 7500 km Sun-Synchronous polar orbit, 10° ahead of the terminator, before subsequent manoeuvring into the 100 km parking orbit. This capture spiral takes 28 days and is shown in Fig. 12, arriving on orbit on March 24, 2017.

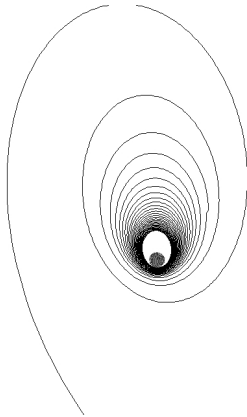


Figure 12: Mercury capture spiral into 100 km x 7500 km Sun-Synchronous polar orbit

131 days will be available for orbital science operations, surface observation and final manoeuvring to the lander descent orbit. This orbiter stay-time is also a requirement due to the thermal environment on the surface. The thermally-benign, Sun-Synchronous orbit (10° ahead of terminator) is forced for 44 days until the orbit is in the correct orientation for the landing site. The sail then waits in this orbit for 37 days. Next, a 50 day manoeuvre transfers the spacecraft to the 100 km polar orbit, where the lander begins its descent on August 3, 2017. Once on the surface, the lander carries out 4 days of sample acquisition and landing site documentation operations. The solar sail is used to rotate the orbit plane to account for Mercury landing site rotation, so that the MAV ascends in a coplanar manoeuvre. The orbit plane cannot be rotated as fast as Mercury spins, so the MAV will need to wait in the 100 km orbit (thermally-safe) until solar sail rendezvous with the MAV. Final proximity manoeuvring is accomplished with the SRV, thereby relaxing MAV launch accuracy. Rotation of the orbit plane to match that of the landing site is depicted in Fig. 13. After sample transfer to the Earth Return Vehicle attached to the sail, the solar sail spirals to

escape. A method which maximises the rate of change of orbit energy while maintaining a positive altitude of periapsis is illustrated in Fig. 14. The escape spiral is initiated on August 18, 2017, with escape reached in 16 days.

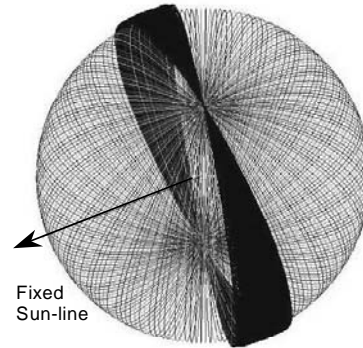


Figure 13: Rotation of 100 km polar orbit plane to match coplanar MAV ascent trajectory

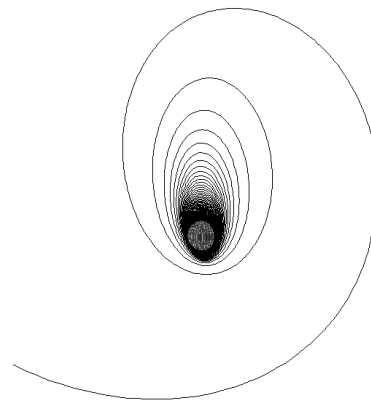


Figure 14: Mercury escape spiral from 100 km circular polar orbit

Mercury-Earth Phase

Return heliocentric spiralling commences after Mercury escape on September 3, 2017. The trip time is 369 days, with arrival back at the Earth with zero hyperbolic excess on September 8, 2018. Fig. 15 shows the 2 revolution trajectory, which is faster because the sail characteristic acceleration has increased to 0.78 mm s^{-2} . The cone and clock angle control profile is shown in Fig. 16. Finally, the ERV spins up and is separated to perform a ballistic entry for sample delivery to Earth. The total mission duration is 4.39 years.

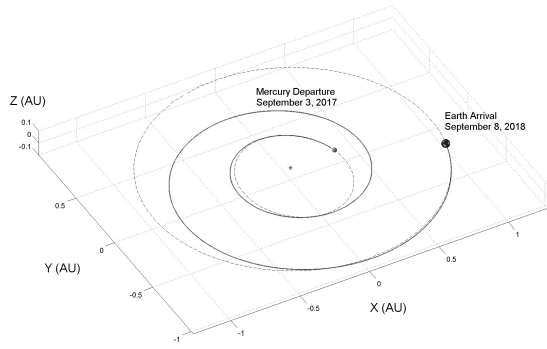


Figure 15: Mercury-Earth trajectory

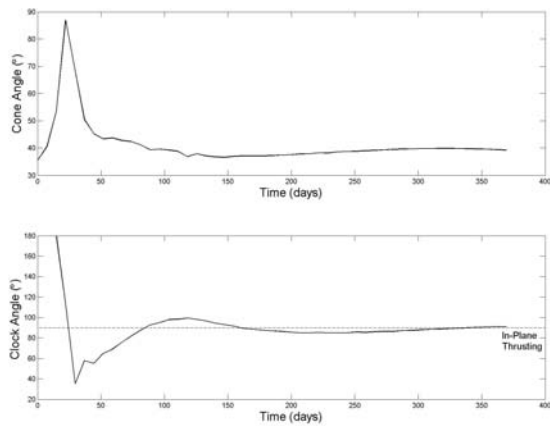


Figure 16: Mercury-Earth control angle profile

Alternative trajectory Options

Use of a positive launch C_3 against the Earth's velocity would be highly advantageous for reaching close solar orbits such as that of Mercury. The initial eccentricity for the inward spiral can be easily circularised by the increased solar radiation pressure closer to the Sun. Fig. 17, shows the effect of using excess launch energy to reduce the trip time to Mercury orbit. It can be seen that the effect is greater for lower accelerations, since the trip time is longer and there are more revolutions for $C_3=0$. The use of a Zenit 3-SL over an H2A, would allow for a $C_3 = 8 \text{ km}^2 \text{ s}^{-2}$, which would reduce the outbound trip time by 260 days, for the same launcher cost.

Fig. 18 shows that the inclusion of a Venus gravity assist could reduce the outbound trip time by 140 days (see Ref. 8), but gravity

assists are not essential for solar sails since propellant mass is not an issue.

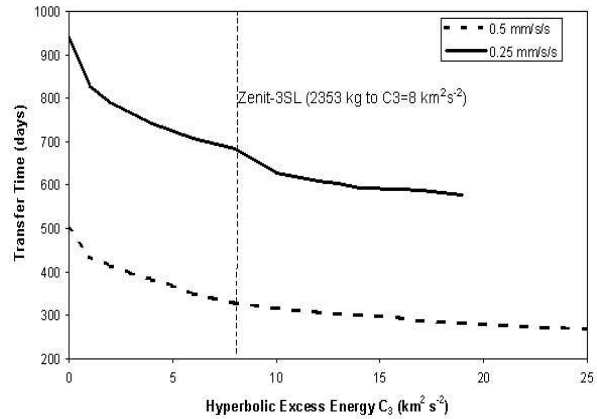


Figure 17: Effect of hyperbolic excess energy at launch

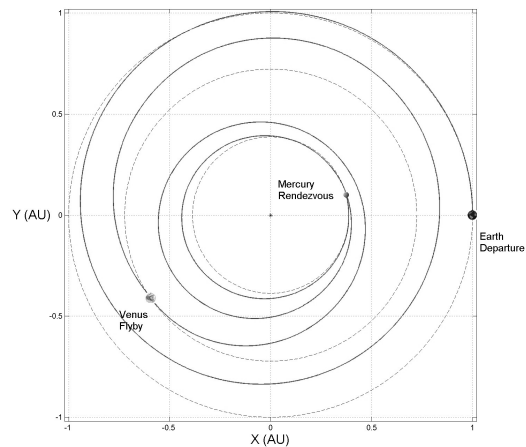


Figure 18: Venus gravity assist

MISSION EVALUATION AND CONCLUSION

Other possible mission architectures were considered in the course of this work.⁴ In addition to the baseline all-sail concept, the use of the sail to spiral to Earth escape to reduce launch energy requirements was considered, a multi-mission concept, and a chemical/sail hybrid mission was briefly investigated. A chemical outbound ballistic transfer to Venus, with a small solar sail deployed for return, is attractive.¹² However, the outbound gravity assisted trajectory to Mercury would dominate the mission duration

of almost 9 years, even though a smaller, cheaper solar sail could be used for the return leg. An Ariane 5 launch would be required in this case.

To summarise the Solar Sail MeSR concept, a 275 m side square solar sail is used to transport a 1905 kg payload to 100 km polar orbit at Mercury, and return a sample to Earth in 4.4 years. The 448 kg, 5.9 g m⁻² solar sail uses AEC-ABLE booms and 2 μm CP1 film, with conventional coatings. The launch mass of 2353 kg is lifted using an H2A202-4S (C₃=0, or Zenit-3 SL to C₃=8). The total mission ROM cost is estimated to be 850 M€.

The mission concept has been compared with other propulsion options.^{1,2} The 5775 kg launch mass of the NASA/JPL Team X SEP concept requires an Atlas V 551 launcher, for a 6.9 year mission, costing of order 1034 M€.² An ESA Chemical/SEP concept has a 6500 kg launch mass on an Ariane 5E, for a mission duration of 7.2 years.¹ No ROM cost is given for this, but it is expected to be in the same order of the NASA cost. Therefore, it is clear that a solar sail MeSR mission can reduce the total mission duration by 40%, and reduce launch mass by 60%, with a reduction in ROM cost of at least 180 M€.

Finally, this analysis assumes the feasibility of large sail structures, their deployment, and attitude control using tip-vanes. There is limited experience of large gossamer structures at present. Therefore, it is imperative that near-term demonstration missions take place, and a rigorous technology development programme is pursued, before a solar sail mission to Mercury can be realised.

ACKNOWLEDGEMENT

This work was performed under ESA/ESTEC contract 16534/02/NL/NR – Technical Assistance in the Study of Science Payloads Transported through Solar Sailing.

REFERENCES

1. Scoon, G., Lebreton, J-P., Coradini, M., et al, "Mercury Sample Return", Assessment Study Report, ESA Publication SCI(99)1, 1999.
2. Oberto, B., et al, "Mercury Sample Return 2002-01," Team X Advanced Projects Design

Team Report, Jet Propulsion Laboratory, Pasadena, California, 2002.

3. McInnes, C. R., *Solar Sailing: Technology, Dynamics and Mission Applications*, Springer-Praxis Series in Space Science and Technology, Springer-Verlag, Berlin, 1999.

4. McInnes, C. R., Hughes, G. W., and Macdonald, M., "Technical Note 3 – Mercury Sample Return," ESTEC 16534/02/NL/NR, ESA/ESTEC Contract Report, University of Glasgow, 2003.

5. Leipold, M.E., Wagner, O., "Mercury Sun-Synchronous Polar Orbits Using Solar Sail Propulsion", J. Guidance, Control and Dynamics, Vol. 19, No. 6, pp 1337-1341, 1996.

6. Murphy, D.M., and Murphey, T.W., "Scalable Solar Sail Subsystem Design Considerations," AIAA 2002-1703, 43rd Structures, Structural Dynamics and Materials Conference, Denver, Colorado, Apr. 22-25, 2002.

7. Wertz, J. R., and Larson, W. J., *Space Mission Analysis and Design*, Kluwer Academic Publishers, pp 795-802, ISBN 0-7923-5901-1, 1999.

8. Hughes, G. W., and McInnes, C. R., "Mercury Sample Return Missions Using Solar Sail Propulsion," IAC-02-W-2.08, 53rd International Astronautical Congress, Houston, Texas, Oct. 10-19, 2002.

9. Hughes, G. W., and McInnes, C. R., "Small-Body Encounters Using Solar Sail Propulsion," *Journal of Spacecraft and Rockets*, Vol. 41, No.1, pp. 140-150, Jan.-Feb., 2004.

10. Macdonald M., and McInnes C. R., "Analytic Control Laws for Near-Optimal Geocentric Solar Sail Transfers," AAS 01-472, Advances in the Astronautical Sciences, Vol. 109, No. 3, pp. 2393-2413, 2001.

11. Macdonald M., and McInnes, C. R., "Seasonal Efficiencies of Solar Sailing in Planetary Orbit," IAC-02-S.6.01, 53rd International Astronautical Congress, Houston, Texas, Oct. 10-19, 2002.

12. Hughes, G. W., Macdonald, M., McInnes, C. R., Atzei, A., and Falkner, P., "Terrestrial Planet Sample Return Missions Using Solar Sail Propulsion," 5th IAA International Conference on Low-Cost Planetary Missions, ESA/ESTEC, The Netherlands, Sept. 24-26, 2003.

- V. Reduced number of different components (space qualification facilitated)
- VI. Reduced launch costs
- VII. More frequent and faster launch possibilities (more recent technologies can be employed)

Although there is a general consensus on the potential for resource reduction through sharing and miniaturisation, there is still a debate about the effectiveness, and the associated risk, if new technologies need to be employed. The benefits from both mission and S/C point of view have been discussed in [5]. For example the Clementine mission to the Moon was built within 22 months according to a microSat concept and has cost only 2/3 of a conventional mission, although it has a rather complex payload [4]. It is also well known that the integration, testing and documentation of missions with payloads comprising discrete separate instruments is tremendous and that interface definition can take years; in fact the mass of the interface control documents exceeds sometimes that of the spacecraft. Since a change in this P/L concept influences the whole chain involving P/L and S/C development including technology issues as well as P/L procurement approaches, it is also highly desirable to understand the impacts of such a new approach. For this reason these aspects of such a system level P/L concept are studied by deriving a preliminary architecture of a Highly Integrated Payload Suite (HIPS) for the BepiColombo Mercury Planetary Orbiter (MPO) with a view to establishing the development, assembly and verification tasks required. This MPO payload serves as a typical example, which could be designed either in a classical manner or using a highly integrated (HIPS) approach and it is used here to mature the resource estimations of the payload of the other mission studies.

2. PAYLOADS OF PLANETARY TECHNOLOGY REFERENCE STUDIES

Technology Reference Studies are mission studies, that are not part of the ESA science program, but which have the purpose to identify the technical development requirements for potential future scientific missions. For planetary exploration, the primary objective is to explore ways to decrease cost and risk by studying the feasibility of small satellite missions, which would allow a phased and systematic approach to the exploration of the planetary bodies of the solar system. The studies were selected to address a wide range of challenging technologies for future exploration of the solar system. The following TRSs are currently under study:

1. **Jovian Minisat Explorer** – a mission to Jupiter’s moon Europa
2. **Venus Entry Probe** – an Aerobot for in-situ exploration of the Venus atmosphere
3. **Interstellar Heliopause Probe** – a probe into the interstellar medium towards the bow shock
4. **Deimos Sample Return** – a zero gravity landing manoeuvre to bring back 1 kg from the moon of Mars
5. **MiniMarsExpress** – small sat mission comparative to Mars Express

This paper describes the aims of these missions with a particular view to the payload requirements and the identification of the pro and cons of the HIPS concept. More details on the complete mission scenario, including S/C, launch, cruise, communication, orbit and their feasibility, can be found in ref. [8,9,10,11]. Similarities of the payload requirements are investigated so as to derive a road map of technology developments which are required to enable the presented mission concepts, where all spacecrafts are to be launched as a single or double composite on-board a Soyuz-Fregat SF-2B launch from French Guyana.

Parallel to these investigations, the HIPS concept and the related instrumentation for the BepiColombo mission is being studied further, thereby serving as a reference to prepare a realistic architecture of the P/L and to be able to compare HIPS to the conventionally implemented and distributed P/L. The status of the design case is beyond the scope of this paper and will be presented elsewhere.

2.1 Jovian Minisat Explorer (JME)

JME consists of two satellites, one of which is used as a relay station for data transmission and the observation of the Jovian system. The second orbiter shall map the moon Europa in a circular orbit at a distance of 200 km. The payload on the Jovian Relay Satellite (JRS), and especially on the Jovian Europa Orbiter (JEO) is constrained by the extreme radiation environment close to Jupiter (up to 5 Mrad after 4 mm Al). Since the instruments face a rather harsh radiation environment, it is recommended to apply radiation hard electronics and to shield sensitive components accordingly.



The main purpose of the JRS payload is the observation of the planet Jupiter and its surroundings during two years, provided the lifetime of the satellite and its payload is long enough. After the payload assessment the following instruments have been envisaged for **JRS**:

Table 1 Resource allocations and purpose of the JRS payload.

Instrument	Purpose	Mass (kg)	Power (W)	Data (kbit/s)
Jupiter Radiation Environment Monitor (JuREM)	Field mapping of the electron and proton activity and its distribution around Jupiter	1.5	1.70	1.1
Jupiter Plasma Wave Instrument (JuPWI)	Plasma wave environment, solar wind interaction with Jovian ionosphere	3.5	1.60	3.75
Jupiter Narrow Angle Camera (JuNaCam)	Imaging and spectroscopy of the surface with 10 different colours.	1.5	1.00	9.1
Jupiter Magnetometer (JuMAG)	Investigation of the Jovian magnetic field	1.15	0.95	0.25
Jupiter Dust Detector (JuDustor)	Measurement of dust present in the Jovian system	1	1.00	0.02
DPU + CPS	Data processing and power supply	2	3.25	-
Shielding (20%)	Shielding of the components	2.13	-	-
Structures	Optical bench and mounting structures	2	-	-
Margin (20%)		2.9	1.9	-
Total		17.7	11.4	14.2

It is intended that the payload shall be embedded in the satellite structure as much as possible. For the payload of JRS, this requirement is slightly relaxed compared to the Europa Orbiter, since the orbit is between 12.7 R_J and 27 R_J . The required effective shielding is only about 5 mm Al equivalent. Nevertheless, the assessment of the available resource revealed that less than 20 kg is available for the JRS payload, which is quite limited for the five instruments. Even more demanding than the low mass requirement is the low power consumption, which is imposed by the low solar flux at the large distance of the Jovian system from the Sun (~5 AU). Analysis has shown that a HIPS approach is the only viable - although still challenging- solution for the selected payload. The mass saving in electronics and the related support structures enables the installation of a payload fulfilling the required performance. One example for resource reduction is the installation of a filter wheel in front of the sensor of JuNaCam instead of in front of the aperture. This allows for a much smaller wheel, compared to a wheel in front of the much larger aperture.

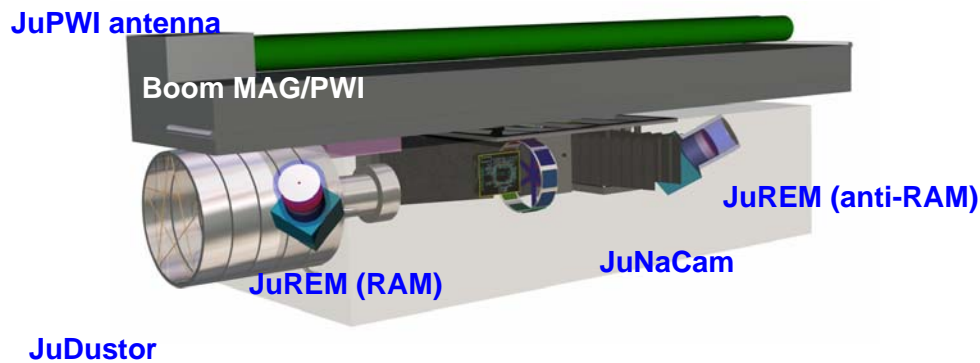


Figure 1 Visualisation of the payload suite. The instruments do not have any demanding requirements on pointing, co-alignment, or thermal requirements and can easily be operated by a central DPU.

The core science of the mission is addressed by the Jovian Europa Orbiter. The main purpose of its payload is the observation of Jupiter's moon Europa during a relatively short period of 60 days. The instruments face a rather harsh radiation environment (5 MRad), requiring a combination of radiation hardened electronics and external shielding to protect sensitive components accordingly. Also here the payload shall be embedded in the satellite structure as much as possible. The following instruments are envisaged for **JEO**:

Table 2 Resource allocations and purpose of the JEO payload.

Instrument	Purpose	Mass (kg)	Power (W)	Data (kbit/s)
Europa Ground Penetrating Radar (EuGPR)	Mapping of the surface and subsurface properties of Europa down to ~20km depth	9.6	20	1.5
Europa Stereo Camera (EuS-Cam)	Stereographic imaging of the surface to derive full topography map	0.6	1.2	5
Europa Visible Near IR Mapping Spectrometer (EuVN-IMS)	Imaging and spectroscopy of the surface at a spatial and spectral resolution of up to 30m/px and 30 nm resp.	2	2	13
Europa Radiometer (EuRad)	Determination of the temperature profiles of Europa in particular at the equator	2	1	0.1
Europa Laser Altimeter (EuLAT)	Topography of the surface and measurement of tidal effects	2	2.5	3
Europa Magnetometer (EuMAG)	Investigation of the presence of a magnetic field of Europa and its interaction with Jupiter	1.4	0.5	0.25
Europa UV Spectrometer (EuUVS)	Mapping of interaction of the ionosphere of Jupiter with Europa	0.5	0.5	TBD
Europa Gamma-ray Spectrometer (EuGS)	Investigation of the elemental surface composition	3	1	TBD
Europa Radiation Environment Monitor (EuREM)	Field mapping of the electron and proton activity and its distribution around Europa	1.5	1	1.1
DPU + CPS	Data processing and power supply	2.5	4	-
Structures	Optical bench and mounting structures	2	-	-
Shielding (20%)	Shielding of the components	5.4	-	-
Margin (20%)		6.5	6.8	-
Total		39	40.5	24

Implementation of ground penetrating radar is particularly demanding. Further savings may be achieved by a light-weight antenna technology. The instrumentation relies on a micro-laser altimeter, a camera with a visible-NIR sensor with broad spectral range and low power requirements throughout, thereby asking for highly miniaturised and integrated electronics.

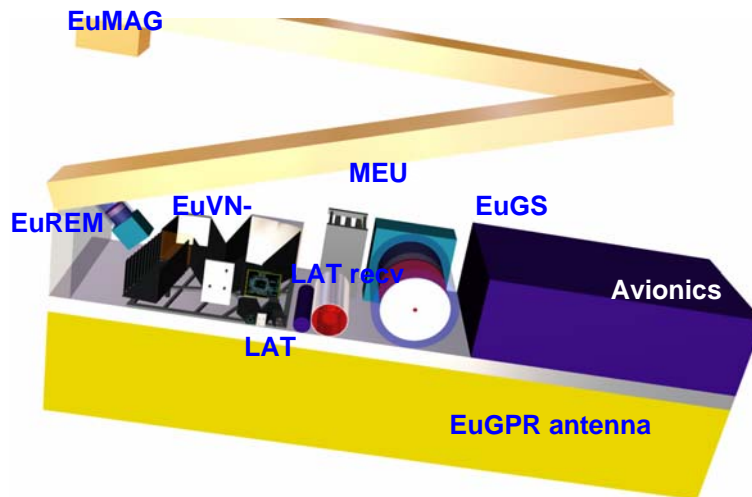
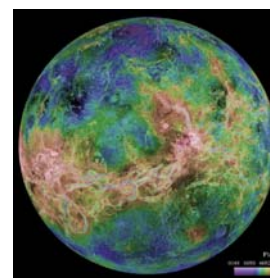


Figure 2 Conceptual layout of the JEO payload. The accommodation is preliminary and will be changed.

2.2 Venus Entry Probe (VEP)

The VEP mission study is designed to undertake the following science investigations:

1. The origin and evolution of the atmosphere by measuring the abundance and isotopic ratios of noble gases
2. Composition and chemistry of the lower atmosphere by determining the minor (<1%) constituents
3. Atmospheric dynamics by accurate measurements of vertical profiles of pressure, temperature and wind velocity
4. Aerosols in cloud layers by measuring the size distribution and temporal and spatial variability of the number density as well as chemical composition
5. Surface and subsurface investigations



These objectives can be summarized as the overall aim to fully understand the atmosphere of Venus in all its aspects and to explore the Venus surface and tectonic structure. The mission scenario that is able to fulfil these objectives consists of two small satellites: the Venus Elliptical Orbiter (VEO) and the Venus Polar Orbiter (VPO) and an Aerobot. The VPO, with the bulk of the atmospheric remote sensing payload, will operate in a polar orbit with altitude at perigee and apogee of about 2000 and 6000 km respectively. This orbit is selected for the study of atmospheric dynamics requiring high spatial and temporal resolution (the orbital period is about 3 hours).

The VEO primarily acts as a data relay station, but will also carry payload more suited to a highly elliptical orbit. The Aerobot will operate at an altitude of approximately 55 km within the Venusian middle cloud layer to derive *in situ* information. The Aerobot design is driven, in particular, by the need to operate in the harsh atmospheric environment of Venus and by a very tight mass budget. During flight, the Aerobot will release small probes which provide height profiles of pressure, temperature, solar flux levels and wind speed.

The VEO operates the following instruments:

Table 3 Resource allocations and purpose of the VEO payload.

Instrument	Purpose	Mass (kg)	Power (W)	Data (kbit/s)
Venus Surface & Subsurface Radar (VSSR)	Surface and subsurface study with high resolution.	12	40	14
UV/ visible camera	UV-CAM2 / tracking of UV features of cloud layers.	1	1	-
DPU + CPS	Data processing and power supply	2	2	-
Margin (20%)		3	8.6	
Total		18	51.6	21

The VEO carries the radar instrumentation for (sub)surface investigations, which has a limited operational altitude, and a UV/visible camera for obtaining images of the complete globe at far distances. Though the topology has been completely and accurately mapped, the subsurface has never before been sounded.

The payload selection for VPO is driven by the penetration characteristics of radiation through the atmosphere. TIR and UV radiation can only provide information on the upper part of the atmosphere and part of the cloud layer. Through NIR radiation, it is possible to observe down to the ground in several NIR window regions. Imaging of the lower atmosphere therefore relies on several of these NIR spectral windows; different spectral channels may probe different atmospheric layers. NIR radiation is also suited to the study of dynamics by monitoring the motion of the cloud layers: while the lower atmosphere is sounded spectrally, cloud opacity can be spatially resolved because the clouds are highly, but conservatively, scattering. The microwave instrument has the attractive features of being able to measure temperature down to around 50 km and to resolve individual spectral lines from which Doppler shifts and hence velocities may be inferred.

Table 4 Resource allocations and purpose of the VPO payload.

Instrument	Purpose	Mass (kg)	Power (W)	Data (kbit/s)
Venus Ultraviolet Spectrometer (VUVS)	Spectroscopy of H ₂ O, SO ₂ , COS, CO, noble gases and unknown UV absorbers; study and mapping of night glow emissions as dynamics tracers; EUV spectroscopy.	4	4	10
Venus UV-Camera (VUVCam)	Tracking of UV features of cloud layers.	1	1	3
Venus Visible Near IR Mapping Spectrometer (VN-IMS)	Tracking of NIR cloud features to study dynamics, esp. super-rotation; monitoring of the O ₂ airglow at 1.27 μm; study of the cloud opacity and its variations; spectroscopy of NIR windows, including search for volcanic activity and study of surface temperature.	4	14	10
Venus IR radiometer (VRad)	Tracking of cloud IR features (especially at poles); H ₂ O mixing ratio; heat transfer; measurements of the outgoing thermal spectral fluxes (radiative balance); temperature/pressure sounding	4	3	10
Venus Micro Wave Sounder (VMS)	CO and H ₂ O mixing ratios, temperature/pressure and wind speed profile from Doppler shifts in limb and nadir views.	6	20	10
DPU + CPS	Data processing and power supply	2	4	-
Margin (20%)		4.2	9.2	8.6
Total		25.2	55.2	51.6

The remote sensing payload will provide new studies in the form of microwave and subsurface exploration and improve upon former studies. The orbit of the VPO offers the possibility of complete global coverage of the upper atmosphere over the length of a super-rotation period (4 days) and a temporal resolution of 3 hours, invaluable for study of the polar vortices for example. Most of the instruments can be miniaturised and well integrated into HIPS, with the exception of the radar instrumentation, largely due to the large antenna. For this reason and the requirement of a low altitude perigee, the ground-penetrating radar is accommodated on the VEO.

The remote sensing measurements of VPO are primarily dedicated to support and enrich the Aerobot investigations. The tentative payload that be integrated into the **Aerobot** and its purpose are given in Table 5:

Table 5 Resource allocations and purpose of the Aerobot payload.

Instrument	Purpose	Mass (kg)	Power (W)	Data (kbit/s)
Gas Chromatograph/Mass Spectrometer (GCMS)	Abundance and isotopic ratios of noble gases, minor gases (e.g., SO ₂ , COS, HCl, H ₂ S and H ₂ O)	0.8	5	TBD
Aerosol analysis package (AAP)	Analysis of particles of Venus' atmosphere	0.3	2	TBD
Solar and IR Flux radiometers (FR)	Measure the radiation transport and heat transfer properties of the atmosphere	0.2	1	TBD
Meteorological package (MP)	Pressure, temperature, light level, flux, acceleration	0.5	1	0.3
Inertial package (IP)	Measure acceleration and changes in attitude	0.05	1.2	
Radar altimeter (RALT)	Determine the position of the Aerobot	0.9	10	
DPU	Data processing	0.25	0.25	-
Structures	Optical bench and mounting structures	0.3	-	-
Margin (20%)		0.7	4.09	
Total		4.0	24.95	TBD
Total (incl. duty cycle)		4.0	5.15	TBD

For reasons such as mass distribution and to be able to keep the option to observe the atmosphere on both sides of the Aerobot, the payload has been split into two HIPS, which are fully integrated into the gondola. Here the resources are extremely low, therefore requiring extremely high miniaturisation and integration of the instruments.

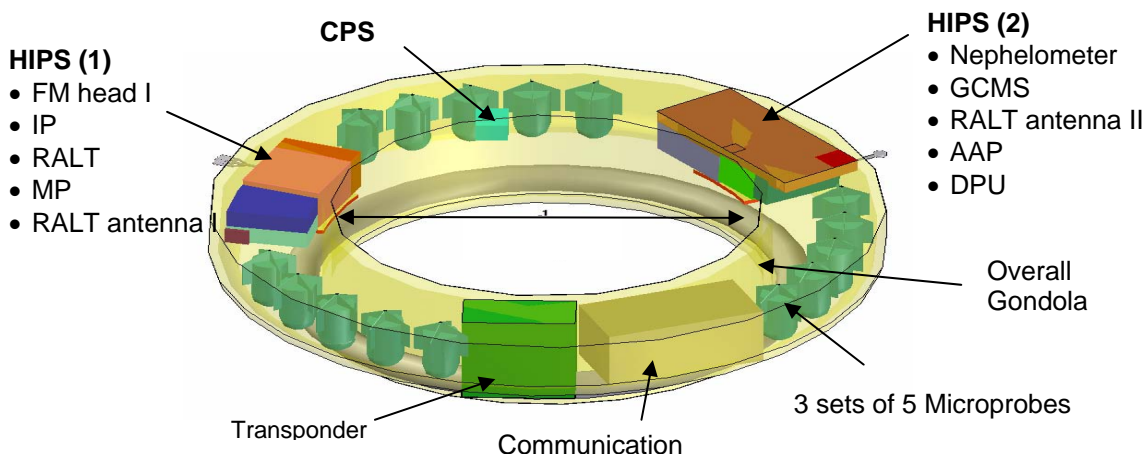
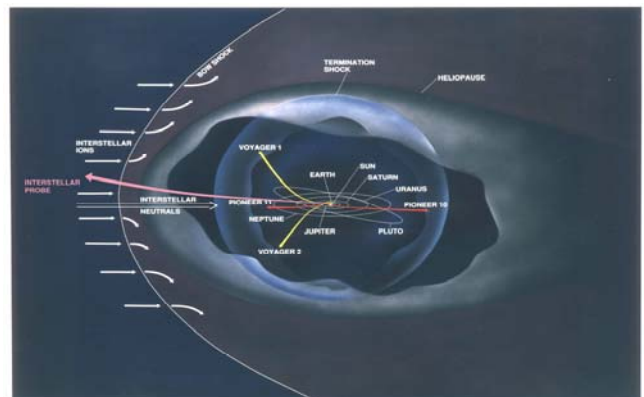


Figure 3 Conceptual design of the payload core of the gondola of the Aerobot with the two envisaged HIPS.

With the exception of the Aerobot, the VEP mission is not particularly constrained by power nor are the mass requirements particularly demanding, although lowering the mass of the VPO payload allows a less eccentric orbit, more suited to the type of global mapping that can unravel the mystery of the Venusian dynamics. Thus in this case, the introduction of the HIPS concept mainly allows an enhancement of the instrument performance and thereby the scientific objectives through resource savings.

2.3 Interstellar Heliopause Probe (IHP)

IHP is to perform chemical and plasma measurements in the heliosphere, the interstellar medium and the interface region between them. The vehicle shall reach a distance of 200 AU from the sun within 25 years. In order to explore the interstellar medium in the shortest time possible the spacecraft shall travel in the direction of the Heliosphere nose, which is located at 7.5° latitude and 254.5° longitude in ecliptic coordinates. In order to minimize the attitude manoeuvring a spinning spacecraft is envisaged. IHP will be the first spacecraft designed to leave the solar system and to enter the interstellar medium. No direct observations of this region exist today. Hence the main objectives of the IHP will be to:



1. explore and investigate the interface between the local interstellar medium (LISM) and the heliosphere,
2. to investigate the influence of the interstellar medium on the solar system,
3. to investigate the influence of the solar system on the interstellar medium, and
4. to explore the nature of the interstellar medium and the outer solar system and the heliosphere.

Additionally a secondary objective might be to observe Trans-Neptunian Objects (TNO) during cruise.

The main purpose of this payload is therefore the study of plasma, energetic particles, magnetic fields, and dust in the outer heliosphere and nearby interstellar medium with a focus to the investigation of the conditions close to the termination shock. The 3-dimensional characteristic of the heliopause requires in principle observations from multiple sides. Since only one S/C is available it is at least tried to have a large coverage of the observations asking for large field of views of the instruments.

Observations aim at the determination of the composition of the plasma and the determination of particle energies and travelling directions of the plasma. The rather broad range of energies from suprathermal to high energetic GeV particles and even neutral atoms requires a whole suite of instruments. The dust grain composition and directional information shall be investigated in-situ. Remote sensing of the dust and the interstellar clouds shall be enabled by UV, VIS-NIR and FIR measurements. The strawman payload is limited in mass and power to 20 kg and 20 W, respectively. This requires a high degree of miniaturisation, integration and demands resource sharing among all instruments. The limited time for communication and lack of interaction requires highly autonomous instruments and a high degree of data compression. The total mass that can be shipped by solar sailing transportation is less than 20 kg.

Table 6 Resource allocations and purpose of the IHP payload.

Instrument	Purpose	Mass (kg)	Power (W)	Data (bit/s)
Interstellar Plasma Analyser (IPA)	Determine the elemental and isotopic composition of plasma and the associated energy levels at temporal composition	2	1	10
Interstellar Plasma Wave and Experiment (IPWE)	Determine the plasma and radio wave environment in outer space CO	5.5	2.5	23
Interstellar Magnetometer (IMAG)	Magnetic field measurements in very low fields	3.2	2.5	8
Interstellar Neutral and Charged Atom Detector and Imager (INCADI)	Energy levels, composition, mass, angular and energy distribution of neutral atoms	0.5	1	16
Interstellar Energetic Particle Detector (IEPD)	Measure supra-thermal, and energetic ions and electrons energy distributions	1.8	1.2	14
Interstellar Dust analyzer (IDA)	Determine the energy levels of cosmic rays	1	0.5	1
Interstellar UV photometer (IUVP)	Surface and subsurface topology with high resolution, altimetry	0.3	0.3	10
Interstellar Visible NIR Imager (IVI)	Determine the radial distribution of Small Kuiper belt objects and TNO	1	0.5	10
Interstellar FIR Radiometer (IFIR)	Measurement of the radial distribution of dust and the cosmic infrared background	0.3	0.2	1
DPU + CPS	Data processing and power supply	2	3.5	-
Structures	Optical bench and mounting structures	2	-	-
Margin (20%)		3.92	2.64	18.6
Total		23.52	15.84	111.6

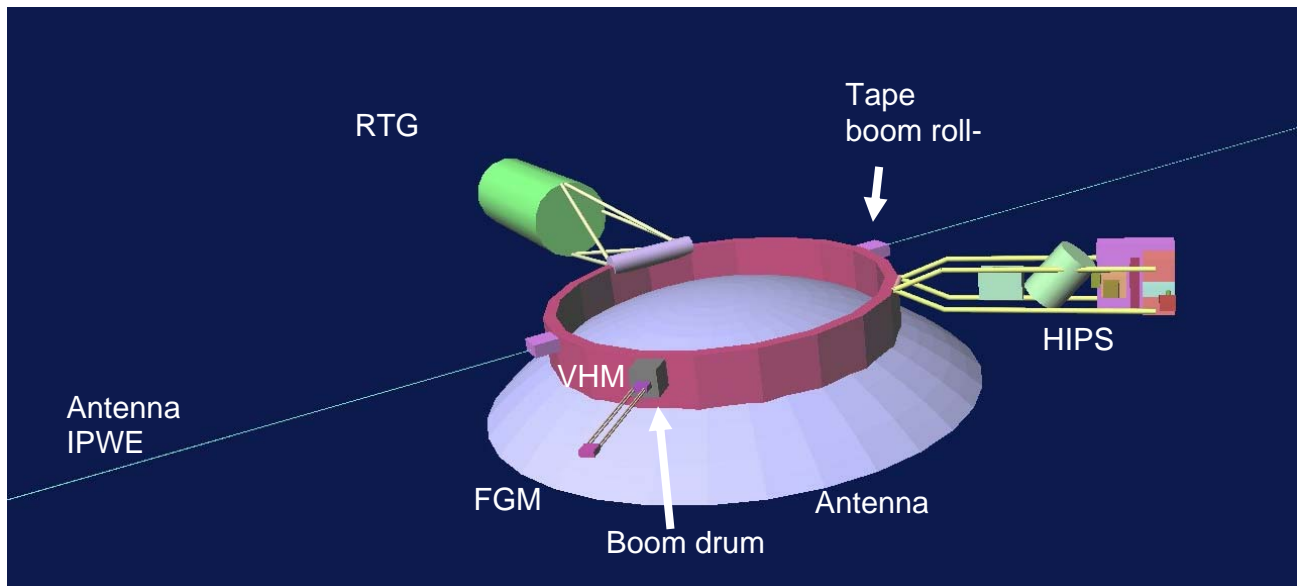


Figure 4 Potential S/C accommodation as far as the payload is concerned. S/C units not included.

2.4 Deimos Sample Return

Two MicroSats launched as a single composite from a Soyuz-Fregat SF-2B shall be inserted into Mars Orbit. One MicroSat acts as a Data Relay Satellite and return vehicle for a Deimos sample and return capsule. The second MicroSat will rendezvous with Deimos to perform a 1 kg sample capture and return to the data relay satellite, which will then leave Mars orbit for a return to Earth, where the capsule will perform a direct re-entry. In the intended single MicroSat scenario, the operations of both satellites are combined aboard one spacecraft. The payload consists as a minimum of a landing system, which allows imaging of Deimos and a distance measurement with the aim to derive landing coordinates and terrain information. Other scientific objectives are the determination of Deimos' size, shape, orbit, gravitational field, rotational properties, surface features and composition. A sufficiently small landing system would allow implementing also some scientific instruments, which could be beside the camera a NIR spectrometer, a UV spectrometer and a scanning system which allows the topographical mapping of the moon. The payload is still under assessment; therefore Table 7 is only indicative.



Table 7 Resource allocations and purpose of the DSR payload.

Instrument	Purpose	Mass (kg)	Power (W)	Data (kbit/s)
μ Stereo Imaging Laser Altimeter (μ SILAT)	Landing coordination, surface topography, shape, size; measure mineralogical composition of the surface (NIR spectroscopy); measure distance during landing and approach	2	3.5	30
Radio Science Experiment (RSE)	Measure Doppler shift during approach	2	6	1
Magnetometer (MAG)	Search for and map intrinsic magnetic fields	0.5	0.5	1
UV photometer (UVP)	Investigate halo and potential exosphere	0.3	0.5	1
DPU + CPS	Data processing and power supply	1	1	-
Structures	Optical bench and mounting structures	1	-	-
Margin (20%)		1.2	2.3	-
Total		8.2	13.8	33

2.5 MiniMarsExpress

The MarsExpress mission is well known and is taken as reference in order to compare the conventional mission with the same mission instrumentation performance implemented in an advanced highly integrated manner. The resources of the instruments of both mission payload concepts are compared in the following table:

Table 8 Resource allocations and purpose of the MEX(*) and MiniMEX() payload – still preliminary.**

Instrument	Purpose	Mass* (kg)	Power* (W)	Mass** (kg)	Power** (W)
High Resolution Stereo Camera (HRSC)	Stereo mapping of Mars with different colours	21.4	40.4	6	2
NIR spectral imager (OMEGA)	Observatoire pour la Mineralogie, l'Eau, Glace, l'Activite	28.8	47.6	5	15
Planetary Fourier Spectrometer (PFS)	Investigation of the atmosphere of Mars	31.2	45	5	3
UV/NIR spectrometer (SPICAM)	Spectroscopy for the Investigation of Characteristics of the Atmosphere of Mars	4.9	25	1.5	3
Plasma Analyser (ASPERA 3)	Analyser of Space Plasmas and Energetic Atoms	5.95	6.4	4	4
Subsurface Radar (MARSIS)	Radar (Subsurface & Ionospheric Sounding)	15	59	10	15
DPU + CPS	Data processing and power supply	-	-	2	4
Structures	Optical bench and mounting structures	-	-	1	-
Margin (20%)		-	-	6.9	9.2
Total		107.25	223.4	39.7	55.2

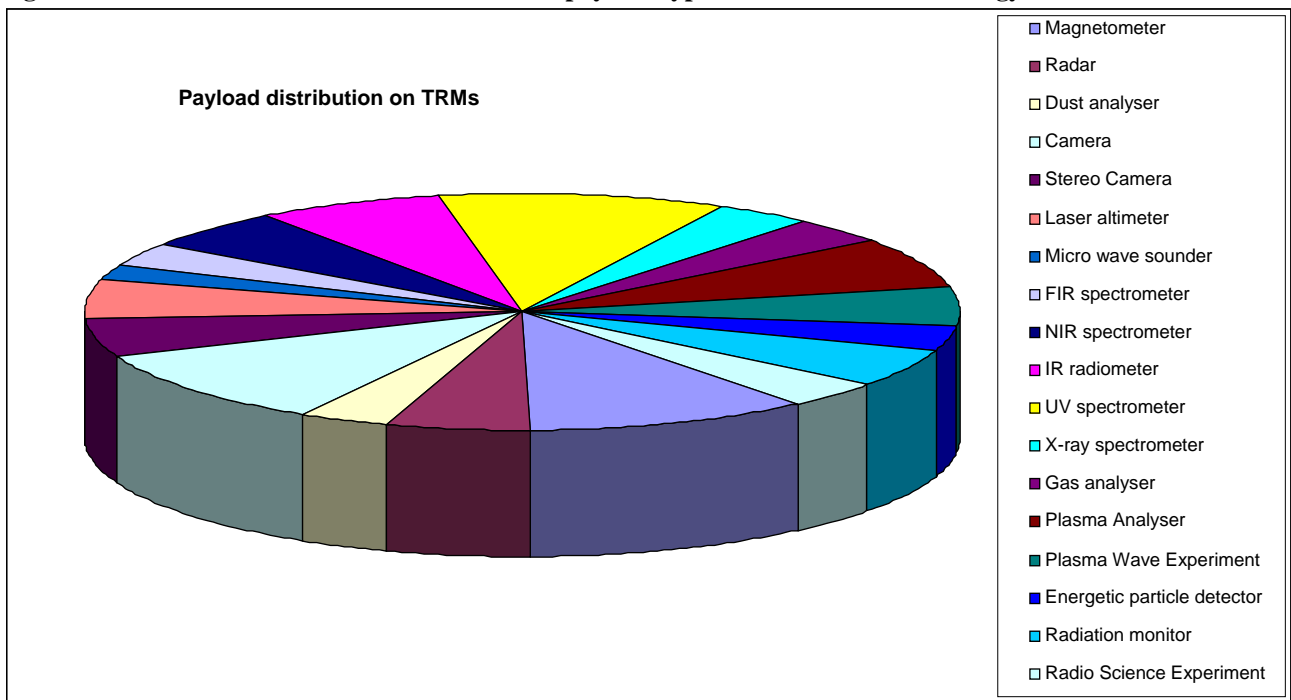
The given resources are preliminary and are still under assessment. The main gain of resources results from the provision of a high performance and centralised DPU, which serves the instruments HRSC, OMEGA, PFS and MARSIS, and from the use of common resources. Instrument concepts and detector technologies are mature for most of the instruments, but must be revisited in the frame of recent developments. It can however already be seen that a saving of about 50% is expected in mass and even 70% in power. Including the snowball effect (multiplication factor of satellite weight for a given increase of payload mass) which is usually ~ 3 , this means that a modern MiniMEX mission would give room for a second S/C being launched with the same rocket and at the same time it would even endorse more or better performing science payload. A new mission to Mars would most likely shift the scope of the scientific instruments, but would still be within the here given resource envelope.

3. GENERIC PAYLOAD

3.1 Instruments

An overview of the payload for all mentioned missions including the payload for the BepiColombo mission shows clearly the need of future technology developments. 18 types of instruments are required in total to cover the scientific demands of the presented 8 orbiters having a total of 52 instruments as strawman payload.

Figure 5 Statistical visualization of the amount of payload types assessed in the technology reference studies.



The highest demand is obviously on magnetometers, cameras and UV spectrometers, and it seems to be feasible that all these instruments can be built from generic components. The ranking of instrument developments according to that chart is the following:

1. Generic fluxgate magnetometers with optional vector Helium magnetometer and miniaturised electronics
2. Cameras being flexible to be changed in aperture size, sensor adaptation and filtering concept with an option of integrating a stereo channel and a laser altimeter
3. UV spectrometers with scalable aperture (photometry is an additional demand)
4. IR radiometer with optional spectrometric capability and broad band spectral range
5. Plasma analyser with possible accommodation of field-of-view

A limited amount of instrument concepts and technologies is needed to realise the observed instrument requirements. The conducted study gives a great insight into the feasibility of building generic instruments or components for scientific space instrumentation, and it allows proposing a roadmap into the future.

3.2 Components

Within the scope of this paper, the particular needs towards generic instrumentation cannot be addressed sufficiently. However, a short list of some of the identified key technologies is given here:

1. Deployable large antennae (subsurface radar)
2. Deployable booms with flexible length for spinning and non-spinning S/Cs (magnetometers)
3. Advanced instrument structures and materials (plastics and lightweight alloys with similar stiffness and thermal conductivity as Aluminium) and their qualification
4. Smart baffles (reflecting thermal heat)
5. Filter technologies (interference filters); perhaps even integrated onto the sensors
6. Optical fibres, and micro-collimators
7. Linear variable and patched filters
8. Sensors being coupled to a passive cooler (radiator)
9. Sensors with low power consumption (CMOS technology)
10. Room temperature bolometers
11. Field Programmable Gate Arrays (FPGAs) and Application Specific Integrated Circuits (ASICs)
12. Highly miniaturised Data Processing Unit (DPU) and bus system

3.3 Electronics

The DPU performance handling different requirements for different missions must be very flexible or scalable. One way to achieve this is to use a scalable processor paradigm such as SPARC (Scalable Processor ARCHitecture). This type of system is designed for use in a multiprocessor system and supports the concept well. With the latest advancements in the LEON core design, this is particularly well suited to a space qualified multiprocessor system approach. There are many approaches to multiprocessor systems, although since recommendations have already been made towards the use of the LEON SPARC-V8 architecture (see Figure 6), which is now followed as baseline. The SPARC concept directly supports the SMP (Symmetrical MultiProcessor) idea which itself has a number of approaches. Two of these approaches include the shared memory multiprocessor, and the distributed memory model. The LEON architecture supports the shared memory model and the SPARC standard supports this directly in its memory model. Specific instructions for multiprocessing are also supported within the SPARC concept, which include atomic load-store operations. IP cores for the implementation of the different functions are made available mostly and considered as generic components.

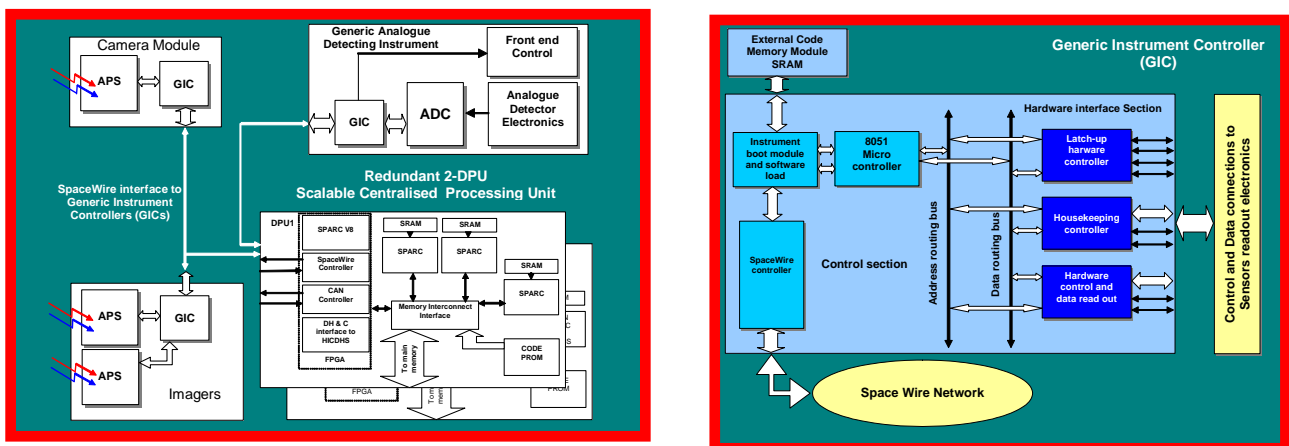


Figure 6 Single Chip Multiprocessor system using LEON SPARC architecture (left) and conceptual layout of the generic instrument controller (right).

The Concept of the Generic Instrument Controller (GIC), allows the central DPU to be able to communicate with all surrounding instruments in the same way. With only minor modifications to the sensor interface, a standard set of functions in the GIC will enable the DPU to “talk” to many differing types of instrument. This will reduce development efforts, not only at the instrument end, but also in the centralised data processing unit. With only one type of interface for communication, the DPU can be highly standardised, and scalable. Many of these system modules can be realised using FPGA technology. Some generic ASICs shall be developed. This also has advantages in mass, size and power consumption. In some cases, whole circuit boards can be replaced by a single programmable component with inter-module connections being simply handled within the device. The processing performance can be adapted from some up to several hundred MIPS while consuming only a few hundred mW.

4. CONCLUSION

Technology Reference Studies are a tool to identify enabling technologies and to provide a reference for mid-term technology developments that are of relevance for potential future scientific missions. Early development of strategic technologies will reduce mission costs and shorten the mission implementation time. As the enabling technologies mature and mission costs reduce, the scientific community will benefit by an increased capability to perform major science missions possible at an increased frequency. The presented technology reference studies have been taken as a showcase for the investigation of the needs on advanced instrumentation for future highly miniaturised and integrated payloads. The term highly integrated is used here not in a literal sense, and is meant more in the sense to provide the basis for a symbiosis being able to benefit from the synergy effects. Instruments can still be distributed and are only combined in case this is subject to a clear advantage. The autonomy of each instrument can still be high, although the ‘central brain’ may observe and command executive payloads. For the presented approach the total payload mass of a satellite is typically around 30kg and weighs therefore as much as single instruments aboard former conventional missions. This might open a new road towards many science driven missions and a future approach for the exploration of the solar system and beyond.

ACKNOWLEDGEMENT

We thank the involved colleagues from ESTEC, EADS Astrium, Surrey Satellite Technology Ltd, Alcatel and Kayser-Threde for the provision of the mission study parameters as far as S/C and orbiter implementation aspects were concerned.

REFERENCES

1. Wertz, James, *Radical Cost Reduction Methods*, in Wertz and Larson (1996), pp. 34–53
2. Wertz, James, and Simon Dawson, *What’s the Price of Low Cost?* paper presented at the 10th Annual AIAA/USU Conference on Small Satellites, Torrance, California: Microcosm, Inc., 1996.
3. Sarsfield L., *The Cosmos in a String*, National Book Network, 2000
4. Bille M., *Microsatellites and improved acquisition of space systems*, Journal of Reducing Space Mission Cost 1: 243–261, 1998 (2001)
5. R. Carli, *System Challenges in the Development of Low-cost planetary Missions*, ESA SP-542 (2003) p. 143
6. M. Collon, *Design and performance of the payload instrumentation of the BepiColombo Mercury Planetary Orbiter*, ESA SP-542 (2003), p. 501
7. S. Kraft, *On the Concepts of a highly integrated payload suite for use in future planetary missions: the example of the BepiColombo Mercury Planetary Orbiter*, ESA SP-542 (2003) 219
8. D. Renton, P. Falkner and A. Peacock, ESA SP-543 (2004), pp. 3-10 (Deimos Sample Return Technology Reference Mission)
9. A. Lyngvi, P. Falkner and A. Peacock, ESA SP-543 (2004), pp. 11-16 (The Interstellar Heliopause Probe)
10. A.C. Atzei, P. Falkner, M.L. van den Berg, A. Peacock, ESA SP-543 (2004), pp. 17-22 (THE JUPITER MINISAT EXPLORER)
11. M.L. van den Berg, P. Falkner, A.C. Atzei, A. Peacock, ESA SP-543 (2004), pp. 23-27 (VENUS ENTRY PROBE)